BULLETIN OF THE EARTHQUAKE
RESEARCH INSTITUTE
Vol. 42 (1964), pp. 533-541

27. *Crustal Structure in Central Japan along Longitudinal Line 139°E as Derived from Explosion-Seismic Observations.*

Part 2. Crustal Structure.

By Hiroshi HOTTA*, Sadanori, MURAUCHI**, Tatsuo USAMI***, Etsuzo SHIMA***, Yoshinobu MOTOYA* and Toshio ASANUMA**.

(Read July 14, 1964.—Received July 30, 1964.)

1. Introduction

This is one of a series of papers under the same title.[1] The crustal structure in Central Honshu in a profile along longitudinal line 139°E will be discussed in this paper, employing observed data on seismic waves from three explosions carried out by the Research Group for Explosion Seismology and described in the first part of this paper. As for the Miyake-zima earthquake, data observed at J. M. A. (the Japan Meteorological Agency) routine stations was used for determining the epicenter.

In the three explosions, the amount of available data obtained was unexpectedly small owing to the complicated character of the crust near the profile on which our observation points were spread, the ineffectiveness of the Kawazu blast, and failure in observing initial motion of artificial seismic waves for the Annaka explosion due to an earthquake which incidentally occurred near Miyake-zima about one minute before the scheduled shot time.

In estimating the crustal structure, only accurate data of first arrivals was employed with reference to S phase and other later phases. However, data at stations north of Nippara (A.10) was employed in the analysis of the Miyake-zima earthquake regardless of its accuracy.

2. Travel times near the shot point

In three explosions, in order to obtain precise knowledge on the

* Department of Geophysics, Faculty of Science, Hokkaido University.
** National Science Museum, Tokyo.
*** Earthquake Research Institute, the University of Tokyo.

1) The Research Group for Explosion Seismology, *Bull. Earthq. Res. Inst.*, **42** (1964), 515-531.

features of the superficial layers near the shot points, several geophones were set up at 3~7 points within about 1 km distance from the shot points. Observed data at these points is shown in Tables 10~12 of Part 1 of this paper and in Figs. 1~3 of Part 2.

Travel time curves calculated by the method of least squares are

SI: $T=0.024+\Delta/1.64$ Siunzi explosion
AI: $T=0.020+\Delta/2.31$ Annaka explosion
KI: $T=0.012+\Delta/2.83$ Kawazu explosion

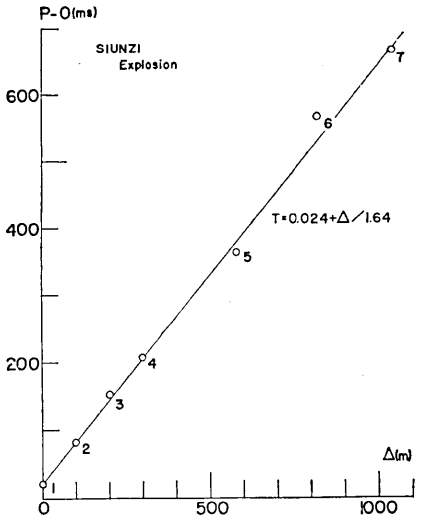

Fig. 1

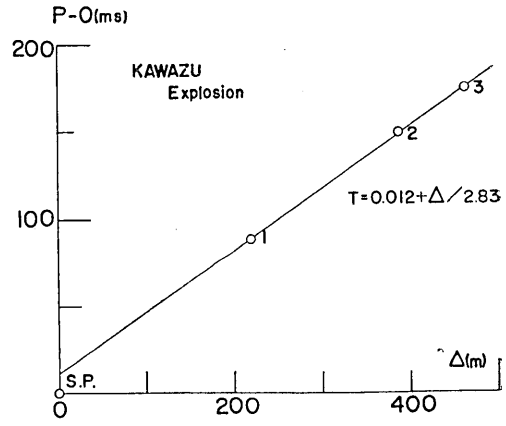

Fig. 2

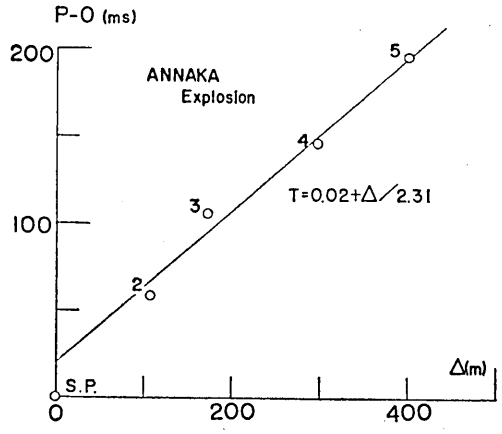

Fig. 3

Fig. 1. Travel time curve near Siunzi shot point.
Fig. 2. Travel time curve near Annaka shot point.
Fig. 3. Travel time curve near Kawazu shot point.

In the numerical computation, equal weight was given to each observed value.

It should be noted that in each explosion the shot time was registered directly on the oscillogram through a lead wire connected to the point adjacent to the electric blasting cap which was buried in the dynamite. Hence, the registered shot time should be correct and the need for considering the delay time is clearly not required.

3. Travel times along longitudinal line 139°E

Travel time curves of the three explosions and the Miyake-zima earthquake are shown in Figs. 4~7. Reduced travel time, $P-O-\Delta/6$,

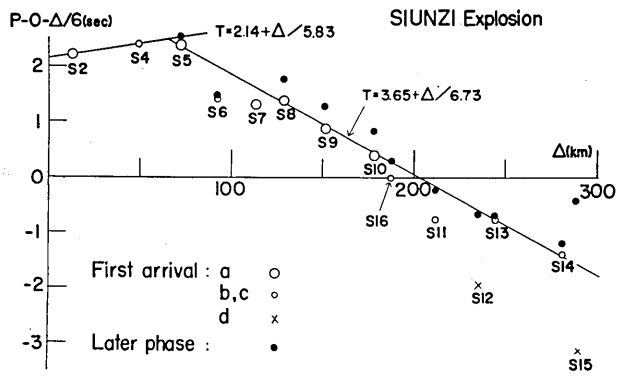

Fig. 4. Reduced travel time curve for Siunzi explosion. In Figs. 4-7, a, b, c and d indicate time accuracy $\Delta t \leqq 0.02$, $0.02 < \Delta t \leqq 0.05$, $0.05 < \Delta t \leqq 0.1$ and $0.1 < \Delta t$ respectively.

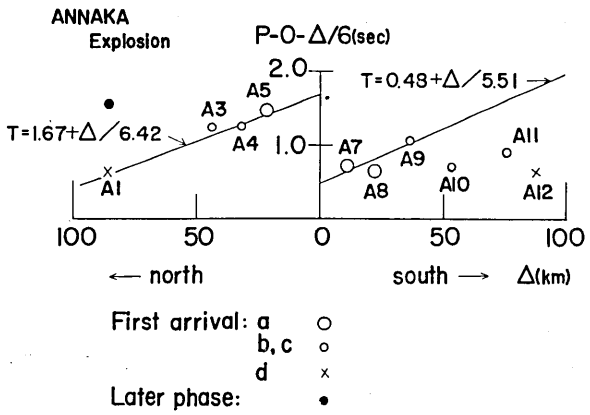

Fig. 5. Reduced travel time curve for Annaka explosion.

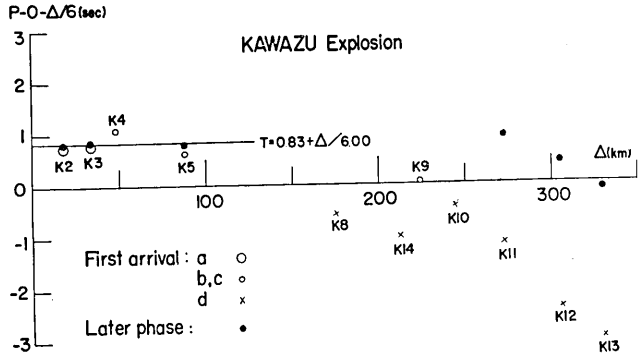

Fig. 6. Reduced travel time curve for Kawazu explosion.

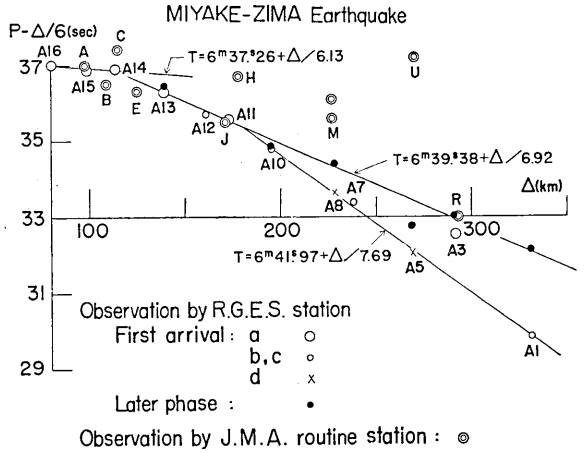

Fig. 7. Reduced travel time curve for Miyake-zima earthquake.

was taken as the ordinate except for the Miyake-zima earthquake in which $P-\Delta/6$ was adopted.

Taking the accuracy of observed values into consideration, the following travel time curves, calulated from the method of least squares, were adopted.

SII : $T=2.14+\Delta/5.83$ Siunzi explosion ($\Delta<75$ km)
SIII : $T=3.65+\Delta/6.73$ Siunzi explosion (70 km$<\Delta$)
AII_N : $T=1.67+\Delta/6.42$ Annaka explosion, northern profile ($\Delta<100$ km)
AII_S : $T=0.48+\Delta/5.51$ Annaka explosion, southern profile ($\Delta<50$ km)
MI : $T=6^m37^s.26+\Delta/6.13$ Miyake-zima earthquake ($\Delta<120$ km)
MII : $T=6^m39^s.38+\Delta/6.92$ Miyake-zima earthquake (110 km$<\Delta<$340km)
MIII : $T=6^m41^s.97+\Delta/7.69$ Miyake-zima earthquake (180 km$<\Delta$)
KII : $T=0.83+\Delta 6.00$ Kawazu explosion ($\Delta<100$ km)

For the Miyake-zima earthquake, data obtained at J. M. A. stations was employed in estimating the epicenter together with that obtained by the Group, but not in calculating travel time curves. $\lambda=139°26'E$ and $\varphi=34°06'N$ was adopted as the geographical coordinates of the epicenter which is located in the area of earthquake swarm[2] which followed the great eruption of the Miyake-zima volcano on Aug. 24, 1962.

Referring to Fig. 4, it seems that a travel time curve with apparent velocity of about 7.3 km/sec can be drawn connecting first arrivals of S16, S11 and S15. However, this curve was not adopted because of the lesser degree of accuracy of observed data.

First arrivals at stations S6 and S7 shown in Fig. 4 are unquestionably clear and appear 0.3～0.06 sec. earlier than the travel time curve SIII.

4. Crustal structure

4.1 Superficial layers

Superficial layers with P wave velocities derived from the travel time curves SI, AI and KI are assumed to exist under the Siunzi, Annaka and Kawazu shot points respectively. Since the shot site for the Siunzi explosion is sand beach in the coast of Niigata Prefecture facing the Japan Sea and this sand layer seems not to extend far inland, the superficial layer with P wave velocity of 1.6 km/sec is assumed to be confined near the shot point and the layer with P wave velocity of 2.31 km/sec, the same as the layer under Annaka shot point, is supposed to exist between Siunzi and Annaka shot points. Furthermore, 6.00 km/sec was adopted as the P wave velocity of the first layer, after referring to the velocities of travel times SII, KII, MI, AII_N, AII_S and our former results in the Kwanto district.[3]

From the above-mentioned assumptions, thickness of the superficial layer under each shot point was estimated, using the intercept time of refracted wave from the first layer, as 2.17 km for Siunzi, 2.09 km and 0.60 km for northern and southern parts of Annaka respectively and 1.33 km for the Kawazu shot points. Structure of superficial layer thus obtained is shown in Fig. 8. Dip angles of the lower boundary of superficial layers were calculated from the apparent velocity

2) 気象庁地震課　三宅島測候所　験震時報 **28** (1964), 別冊, 13-21.
3) T. USAMI et al, *Bull. Earthq. Res. Inst.*, **36** (1958), 349-357.

of waves passing through the first layer and assumed velocities of the first and superficial layers and are shown in the figure. The first layer crops out between S7 and S8 stations. This result is supported by the

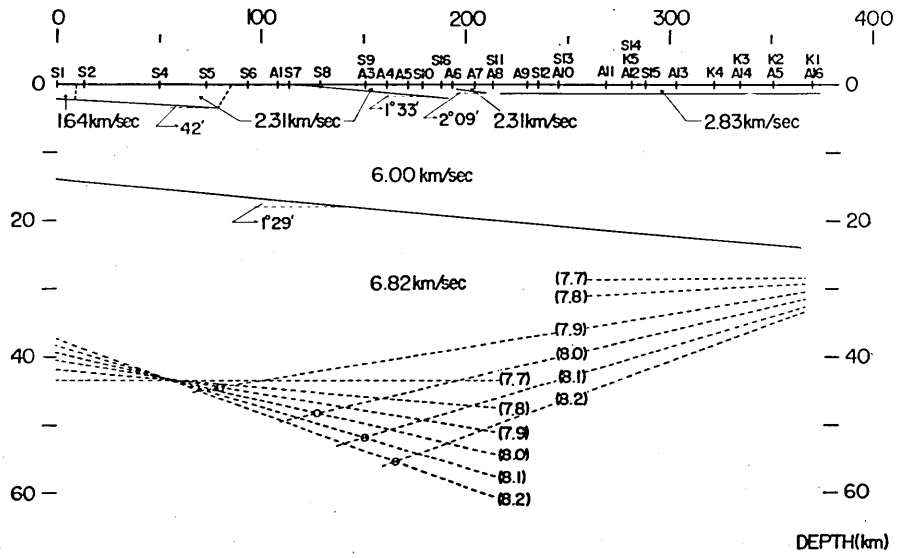

Fig. 8.

first arrivals at S7 and S8 which appeared 0.3～0.6 sec earlier than the travel time curve SIII. The thickness of the superficial layer under each shot point is not sensitive to the change of the velocity of first layer V_1. For example, if we take 5.5 km/sec as the P wave velocity of the first layer, this thickness becomes larger by about one per cent.

4.2 First layer

Since the thickness of superficial layer is not so small and the velocity and thickness change from place to place, the following assumptions are made as to the superficial layer in calculating the thickness of the first layer. As is shown in Fig. 9, it is supposed that the boundary surfaces between V_1 layer and V_0 or V_0' layer are horizontal and the travel time curves SIII and MII are those of seismic waves passing through V_2 layer.

Hence, from the apparent velocities of travel time curves SIII and MII and the true velocity of the first layer, the velocity of the second layer and dip angle of lower boundary of the first layer are given as

V_2=6.82 km/sec and ω=1° 28.5′ respectively.

Adopting numerical values V_0=1.64 km/sec, h_0=2.17 km, V_0'=2.83 km/sec and h_0'=1.33 km and using intercept time of travel-time curve SIII,

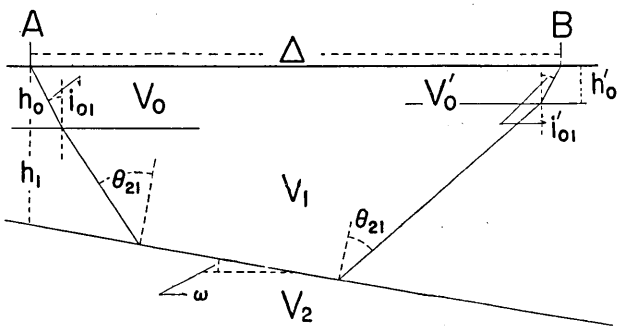

Fig. 9

the thickness of the first layer is obtained as h_1=11.8 km under the Siunzi shot point from which the depth to the lower boundary of the first layer is calculated as $h=h_0+h_1$=13.9 km.

For the range of plausible values of the velocity and thickness of the superficial layer this depth varies between 13~14 km for V_1=6.00 km/sec and between 11~12 km in case of V_1=5.5 km/sec.

4.3 The Mohorovičič discontinuity

Since only the observed data bearing information about the features of the Mohorovičič discontinuity is the travel time curve MIII of the refracted wave passing through the upper mantle, it is inadequate to draw detailed features of this Mohorovičič discontinuity. However, it is not meaningless to estimate approximate features of the discontinuity using the given data.

At first, the following assumptions are made:

1) The layering is horizontal.
2) Superficial layer is homogeneous and 2 km thick with P wave velocity V_0=2.5 km/sec.
3) The first layer is also homogeneous, having P wave velocity 6.00 km/sec and thickness 11.5 km.
4) Hypocenter of Miyake-zima earthquake is situated on the earth surface.
5) Cross-over distance of travel times MII and MIII is 150 km. From

these plausible numerical values and assumptions, the features of the Mohorovičič discontinuity near Miyake-zima were obtained for various values of P wave velocity in the upper mantle and are shown in Fig. 8 by dotted lines on the right. If the thickness of the first layer is 20 km, the Mohorovičič discontinuity becomes deeper by 5 km. Furthermore, when the Miyake-zima earthquake has a finite focal depth, which is the actual case, the Mohorovičič layer becomes deeper.

While, in the Siunzi explosion, seismic waves refracted into the upper mantle was not observed clearly. It is assumed that the Pn wave does not appear at stations nearer than S 14(Δ=281 km), that is, travel times of SIII and Pn, if they exist, cross at epicentral distance Δ=281 km. Furthermore, the apparent velocity of travel time curve of Pn wave is supposed to be 7.7 km/sec.[4] Under these assumptions, the Mohorovičič layer near the Siunzi shot point is obtained and is shown in Fig. 8, for various values of Pn wave velocity, by dotted lines on the left. Numerals in parentheses are the assumed values of P wave velocity in the upper mantle.

5. Concluding remarks

Employing observed data of seismic waves of three largescale explosions and one natural earthquake, crustal structure along the longitudinal line 139°E was estimated. Owing to the lack of information about the wave passing through the upper mantle, only approximate features of the Mohorovičič discontinuity were given.

The existence and features of the second layer with P wave velocity of 6.82 km/sec or so was first ascertained in Japan. If the boundary surface of the first and second layers extends southward maintaining the same inclination, the second layer disappears under Miyake-zima. To ascertain the crustal structure in the Pacific near Miyake-zima is an interesting problem yet to be explored. The tendency of the Mohorovičič layer becoming shallower towards the south is qualitatively acceptable from the viewpoint that the crust is thinner under the ocean than under the continent.

It should be stressed here that observations at further stations and extensions of temporary stations to islands south in the Pacific is necessary to obtain more detailed knowledge of crustal structures in this region.

4) *loc. cit.*, 3).

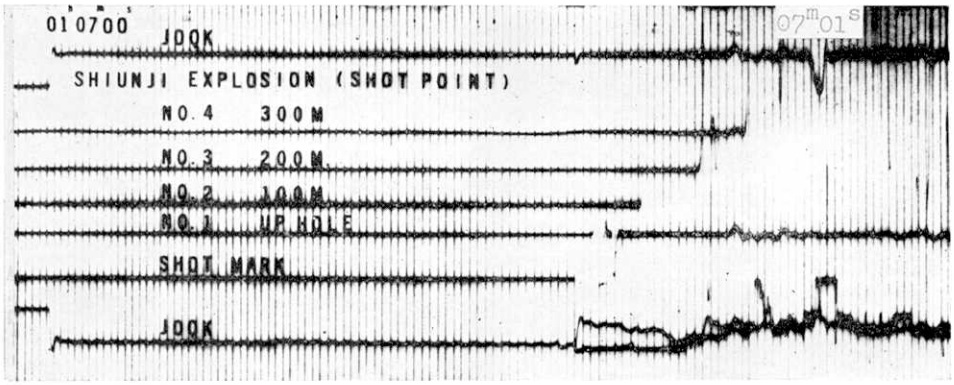

Fig. 5-1. Seismogram obtained at shot point for Siunzi explosion.

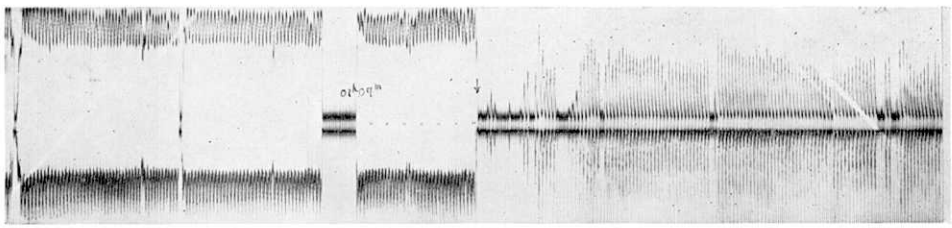

Fig. 5-2. Shot mark of Siunzi explosion recorded on magnetic tape.

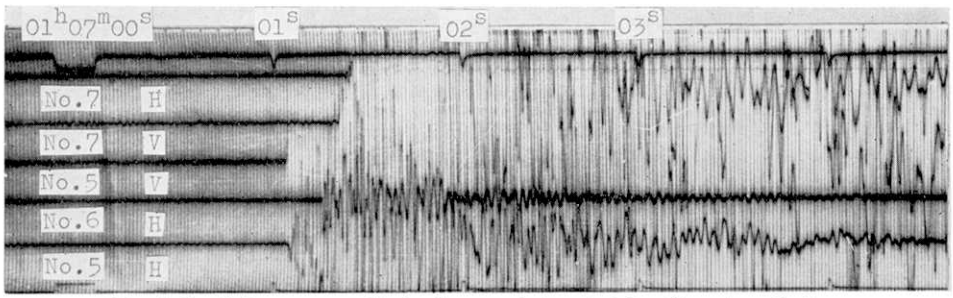

Fig. 5-3. Seismogram obtained near shot point for Siunzi explosion.

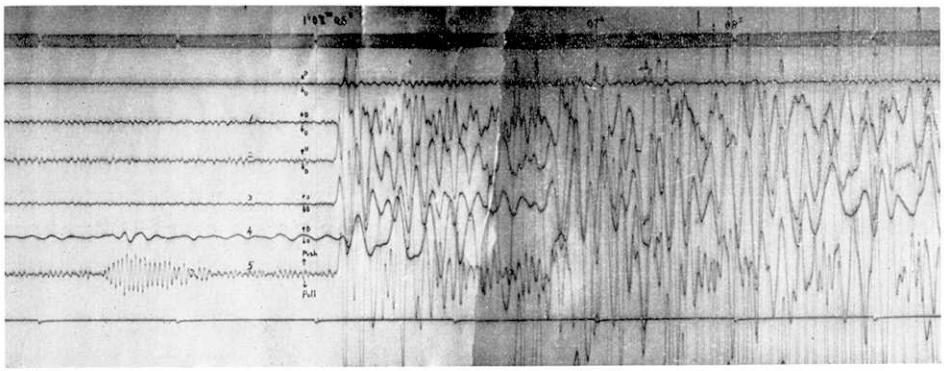

Fig. 5-4. Seismogram obtained at Nakaura for Siunzi explosion.

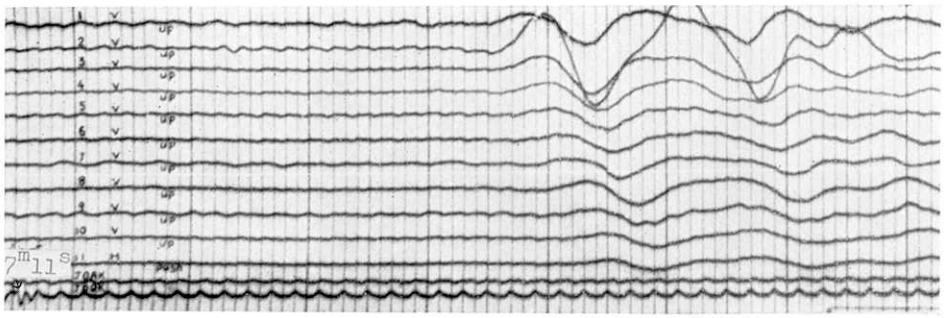

Fig. 5-5. Seismogram obtained at Simotakayanagi for Siunzi explosion.

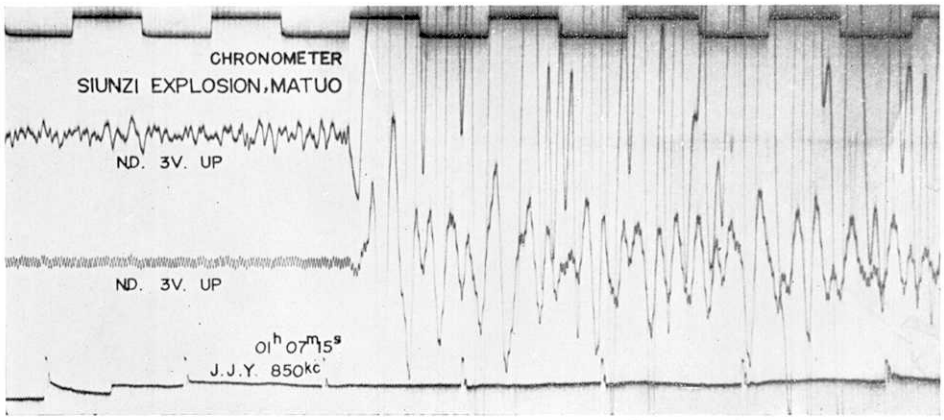

Fig. 5-6. Seismogram obtained at Matuo for Siunzi explosion.

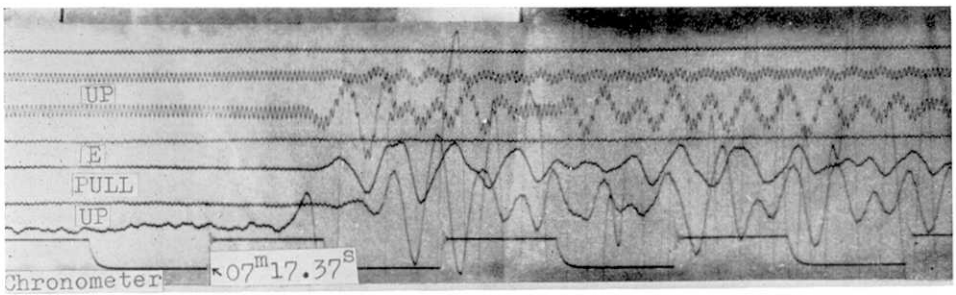

Fig. 5-7. Seismogram obtained at Yunotani for Siunzi explosion.

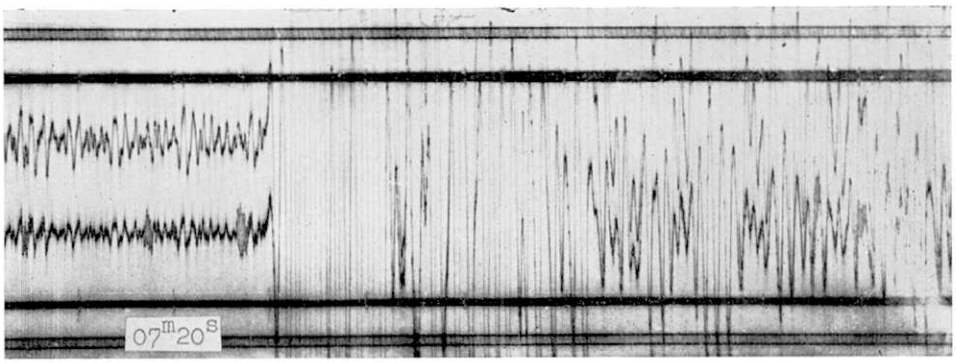

Fig. 5-8. Seismogram obtained at Ikazawa for Siunzi explosion.

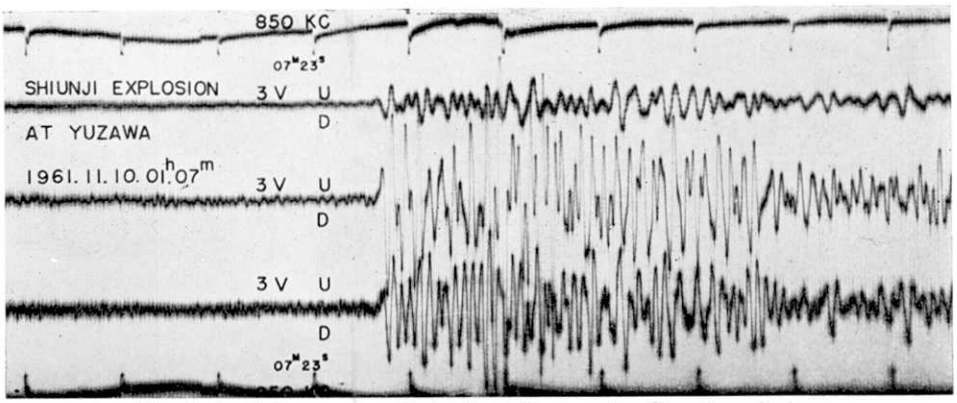

Fig. 5-9. Seismogram obtained at Yuzawa for Siunzi explosion.

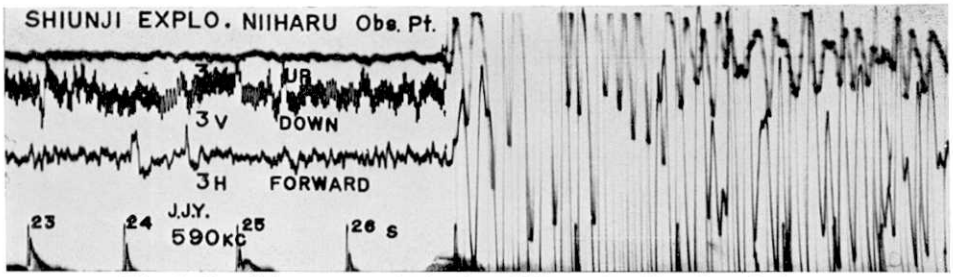

Fig. 5-10. Seismogram obtained at Niiharu for Siunzi explosion.

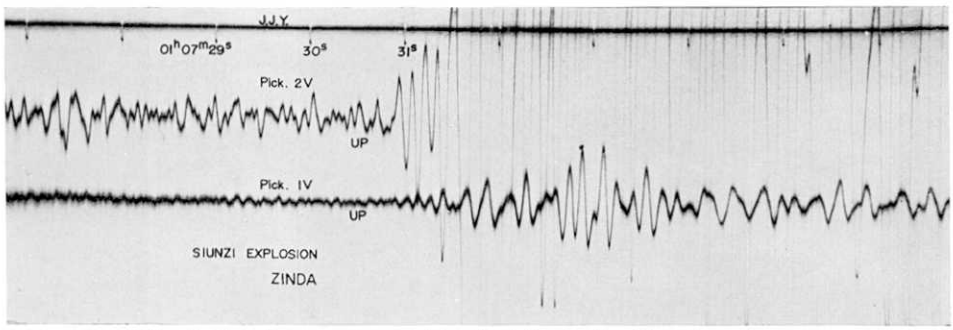

Fig. 5-11. Seismogram obtained at Zinda for Siunzi explosion.

Fig. 5-12. Seismogram obtained at Simokubo for Siunzi explosion.

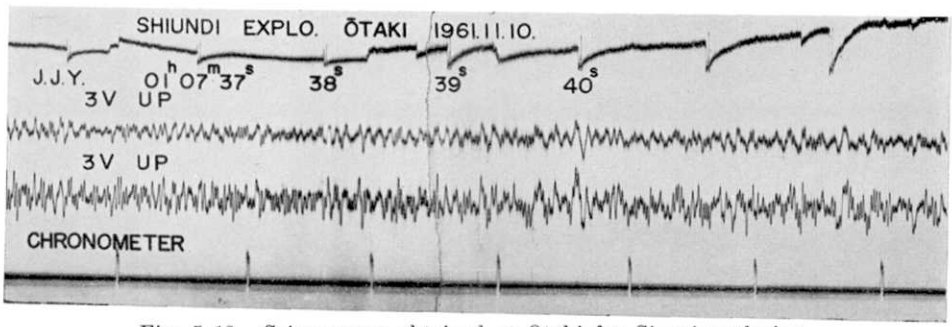

Fig. 5-13. Seismogram obtained at Otaki for Siunzi explosion.

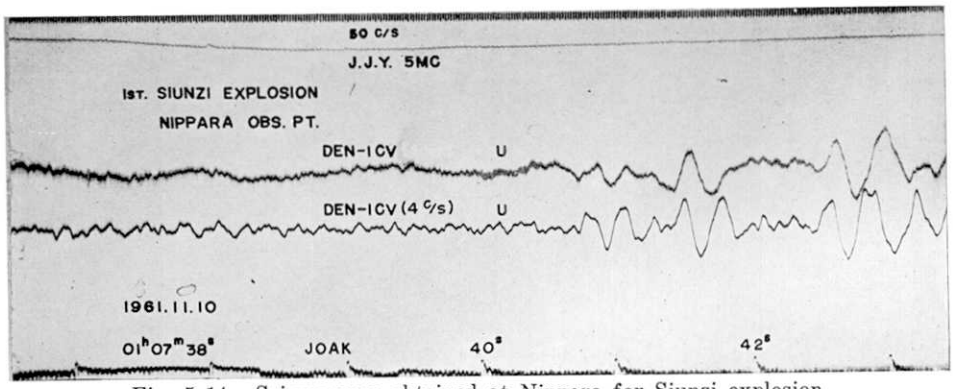

Fig. 5-14. Seismogram obtained at Nippara for Siunzi explosion.

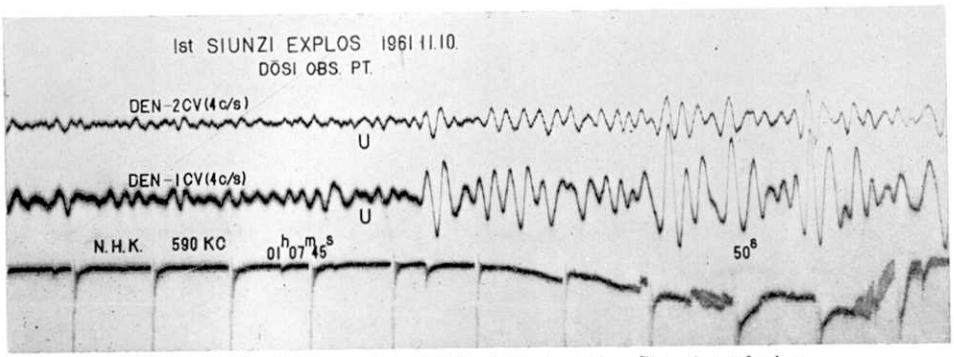

Fig. 5-15. Seismogram obtained at Dosi for Siunzi explosion.

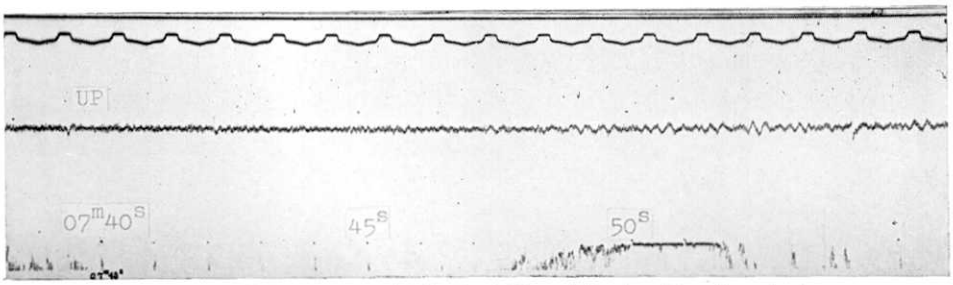

Fig. 5-16. Seismogram obtained at Yamakita for Siunzi explosion.

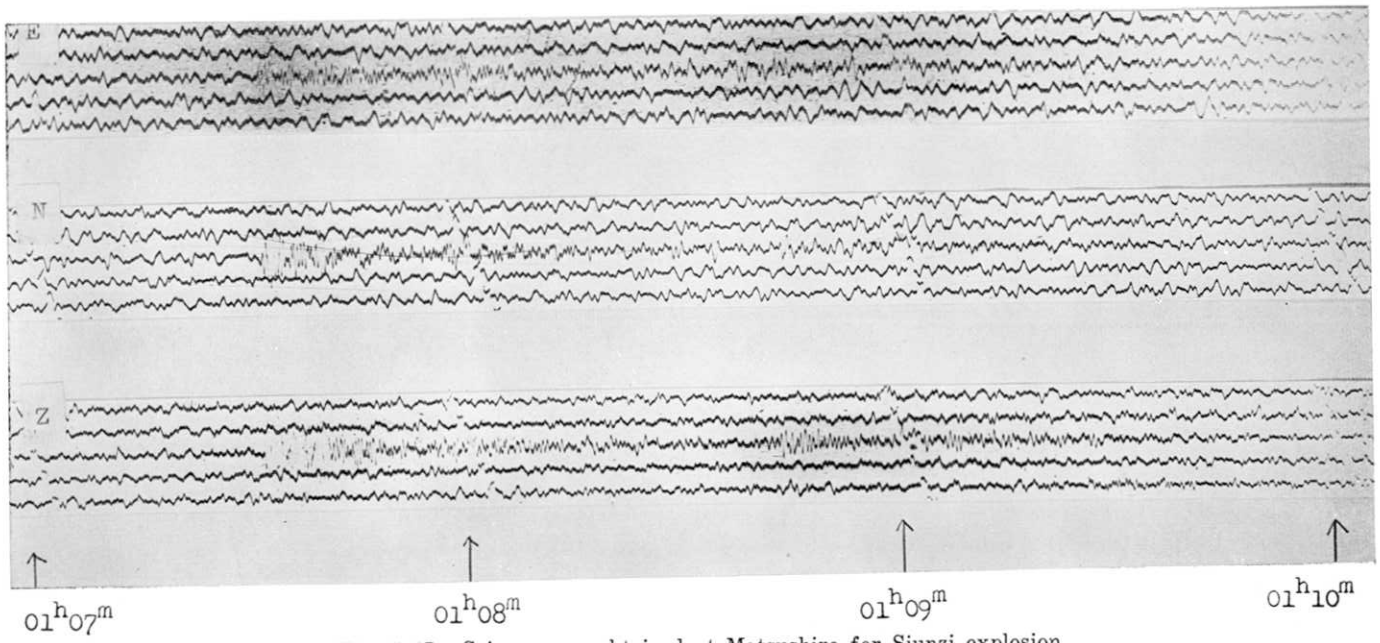

Fig. 5-17. Seismogram obtained at Matsushiro for Siunzi explosion.

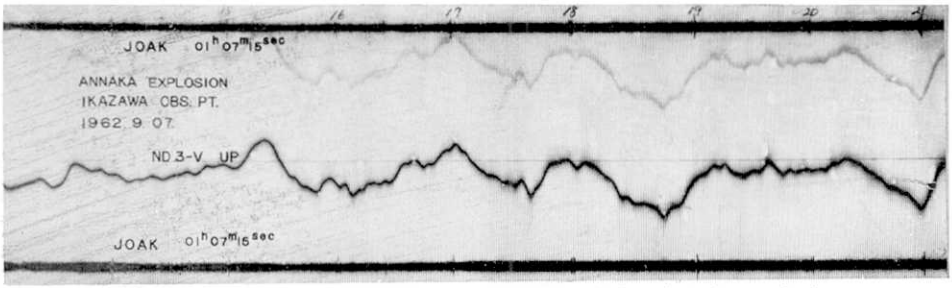

Fig. 5-18. Seismogram obtained at Muikamati for Annaka explosion.

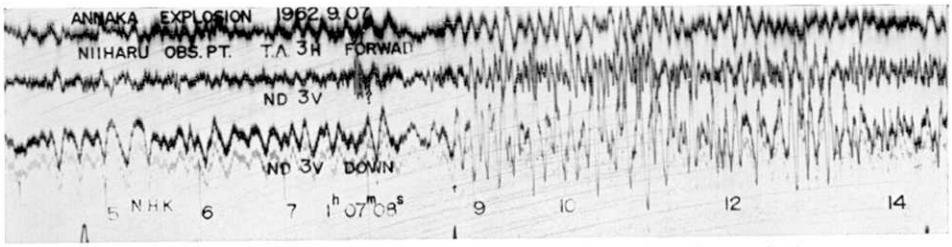

Fig. 5-19. Seismogram obtained at Niiharu for Annaka explosion.

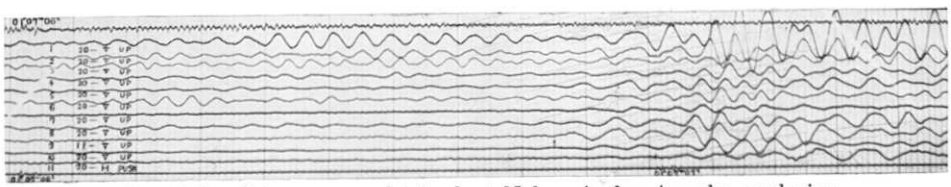

Fig. 5-20. Seismogram obtained at Nakanojo for Annaka explosion.

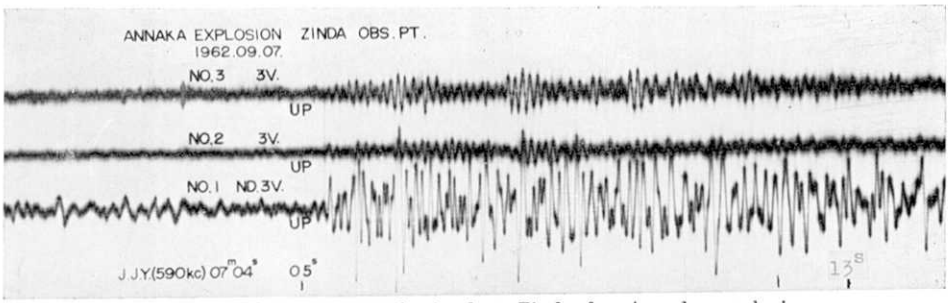

Fig. 5-21. Seismogram obtained at Zinda for Annaka explosion.

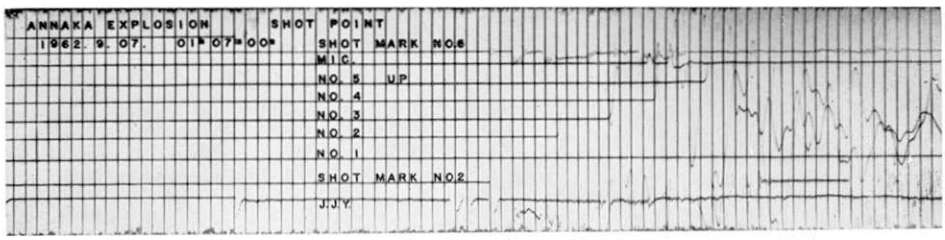

Fig. 5-22. Seismogram obtained at shot point for Annaka explosion.

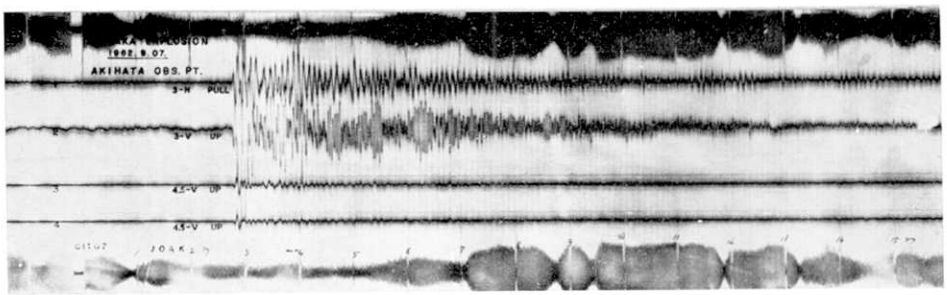

Fig. 5-23. Seismogram obtained at Akihata for Annaka explosion.

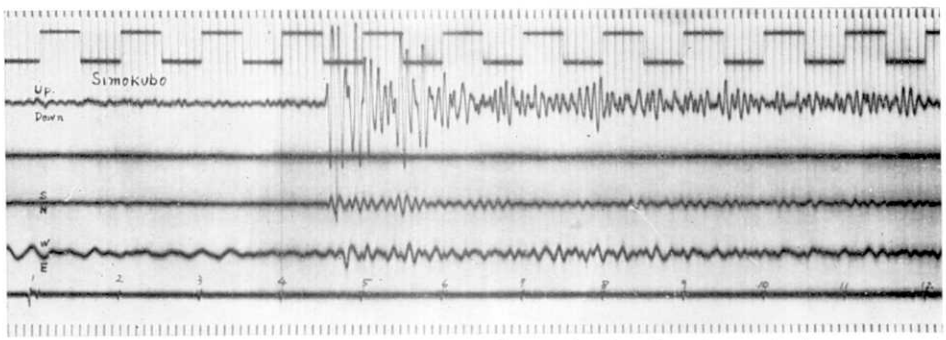

Fig. 5-24. Seismogram obtained at Simokubo for Annaka explosion.

Fig. 5-25. Seismogram obtained at Arakawa for Annaka explosion.

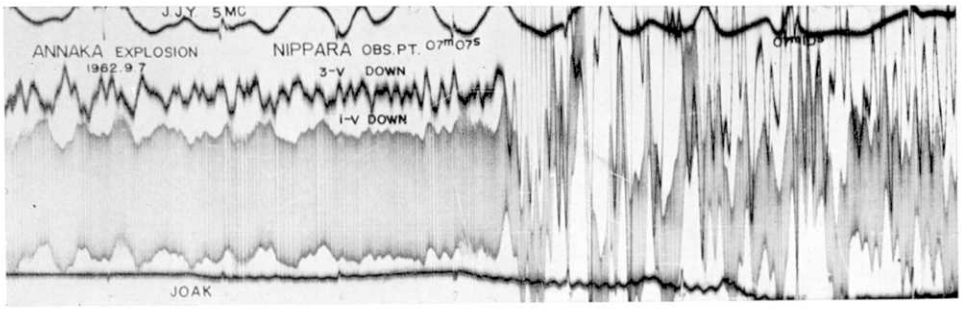

Fig. 5-26. Seismogram obtained at Nippara for Annaka explosion.

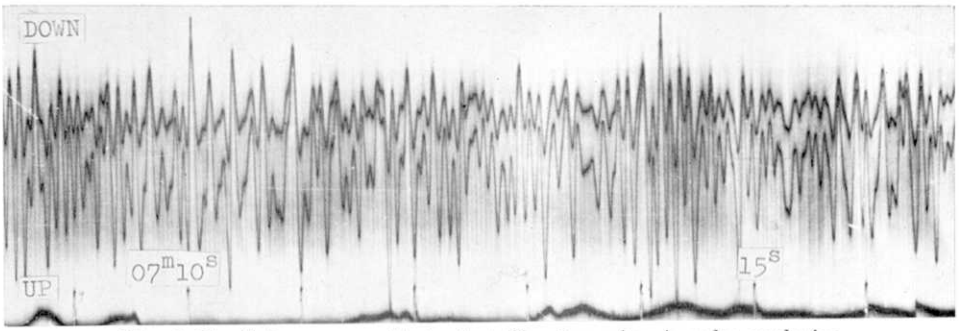

Fig. 5-27. Seismogram obtained at Uenohara for Annaka explosion.

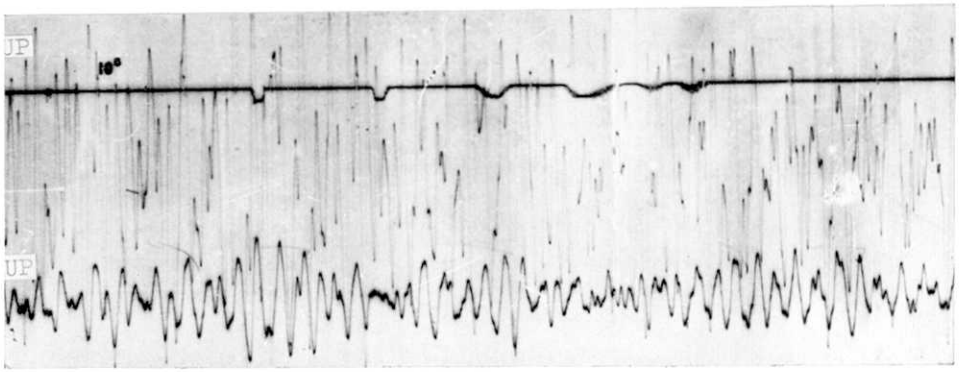

Fig. 5-28. Seismogram obtained at Dosi for Annaka explosion.

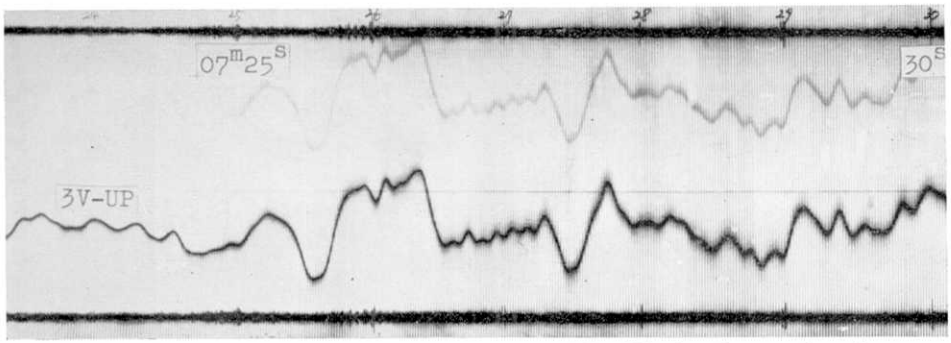

Fig. 5-29. Seismogram obtained at Muikamati for Miyake-zima earthquake.

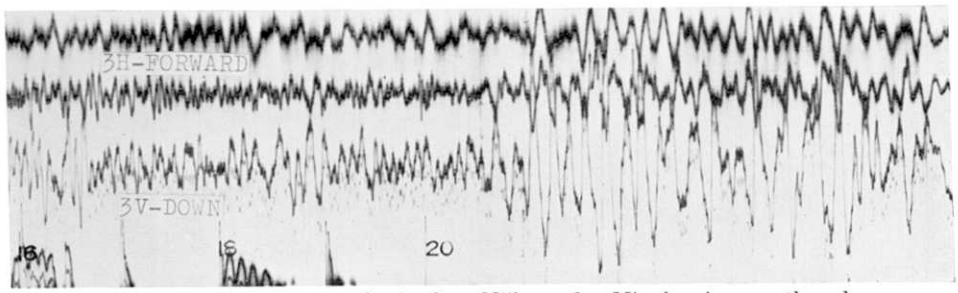

Fig. 5-30. Seismogram obtained at Niiharu for Miyake-zima earthquake.

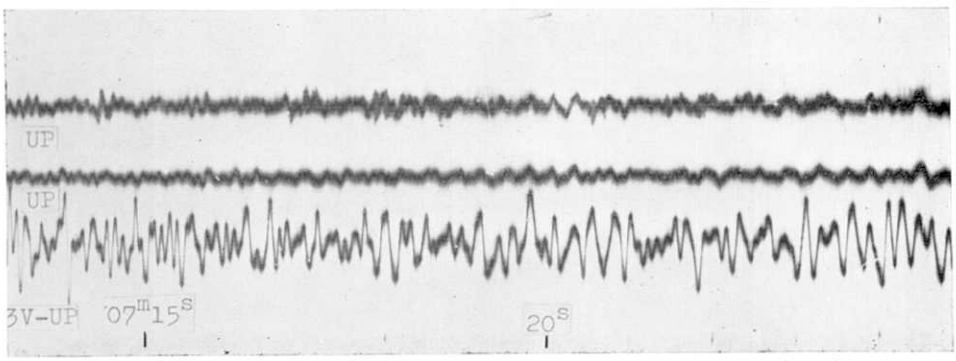

Fig. 5-31. Seismogram obtained at Zinda for Miyake zima earthquake.

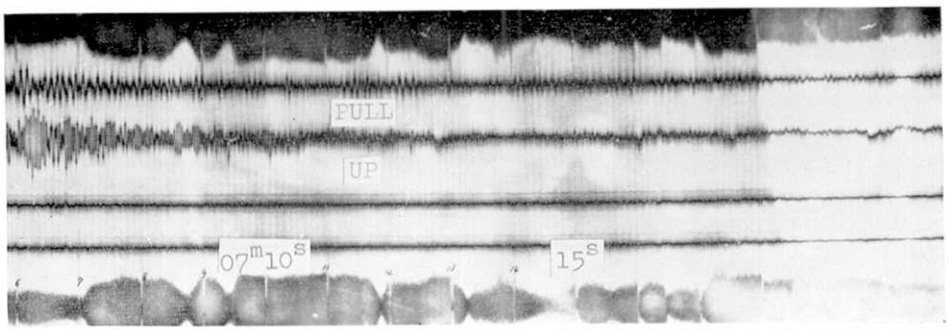

Fig. 5-32. Seismogram obtained at Akihata for Miyake-zima earthquake.

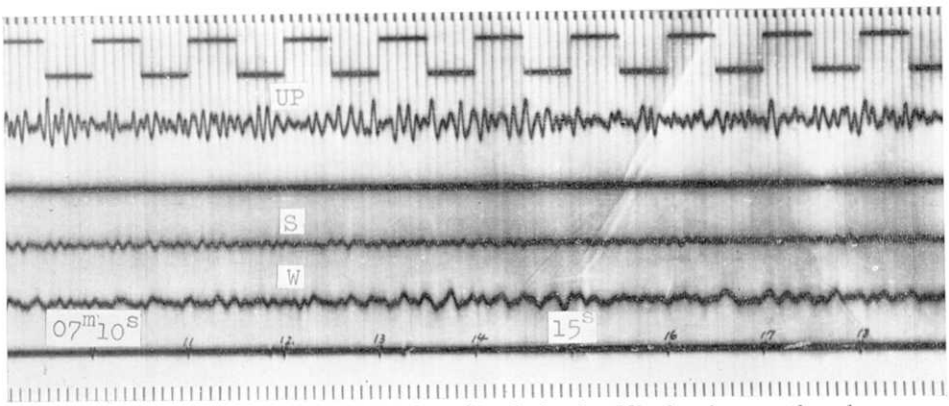

Fig. 5-33. Seismogram obtained at Simokubo for Miyake-zima earthquake.

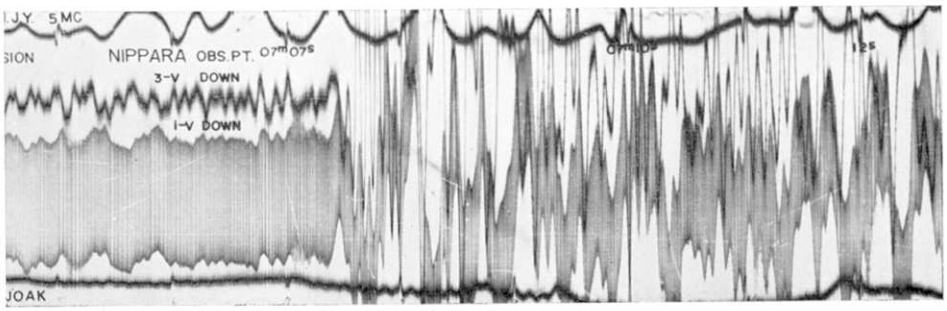

Fig. 5-34. Seismogram obtained at Nippara for Miyake-zima earthquake.

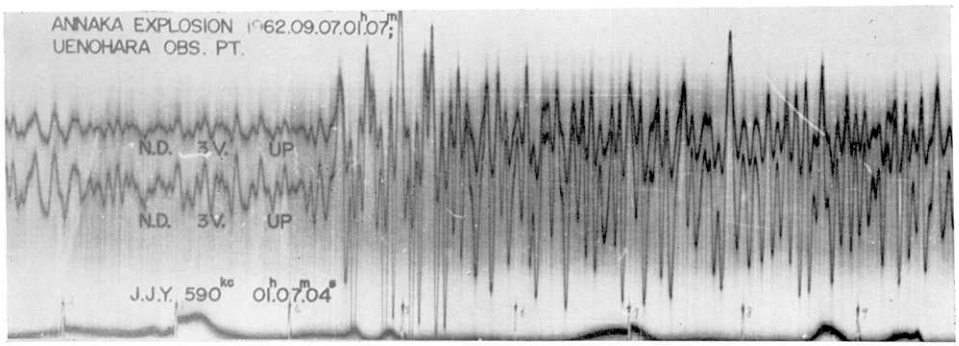

Fig. 5-35. Seismogram obtained at Uenohara for Miyake-zima earthquake.

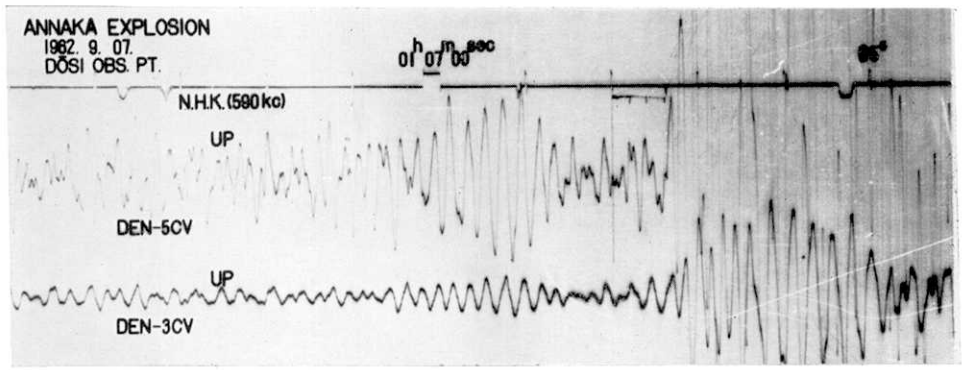

Fig. 5-36. Seismogram obtained at Dosi for Miyake-zima earthquake.

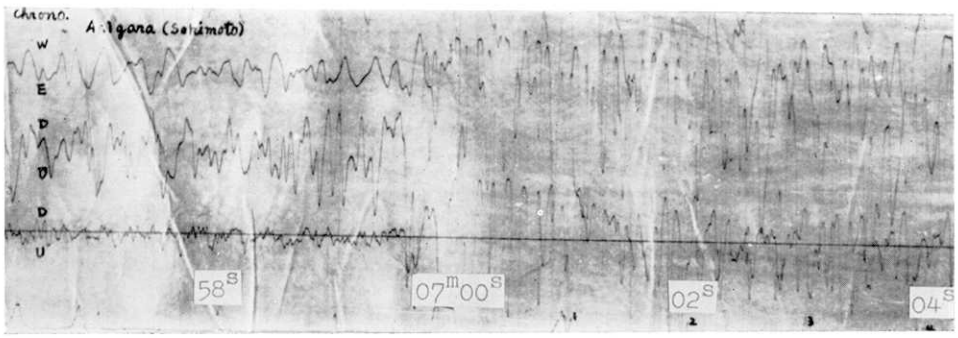

Fig. 5-37. Seismogram obtained at Asigara for Miyake-zima earthquake.

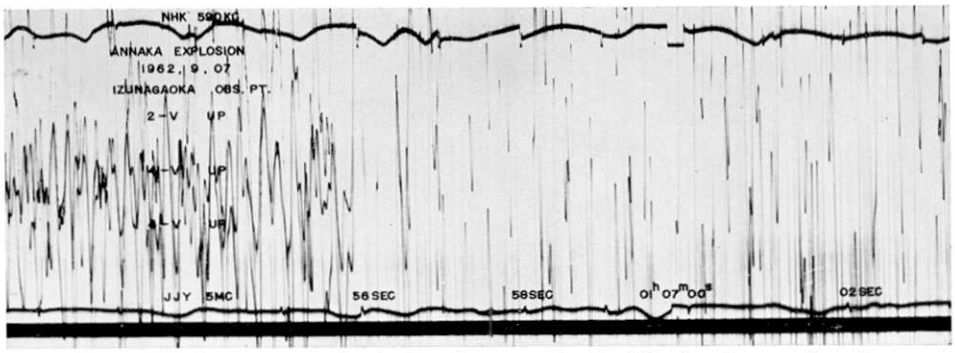

Fig. 5-38. Seismogram obtained at Izu-nagaoka for Miyake-zima earthquake.

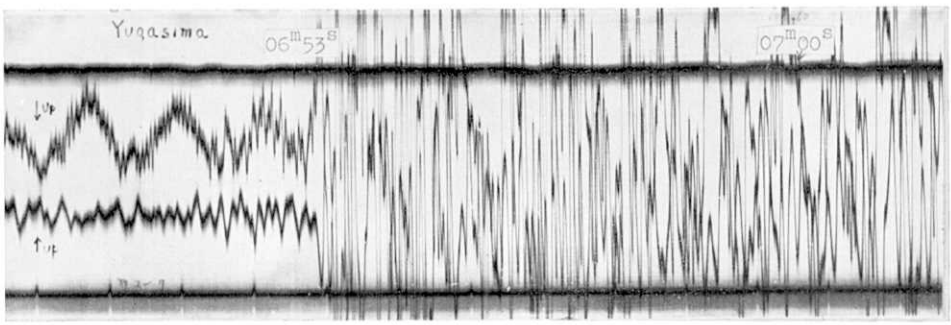

Fig. 5-39. Seismogram obtained at Yugasima for Miyake-zima earthqake.

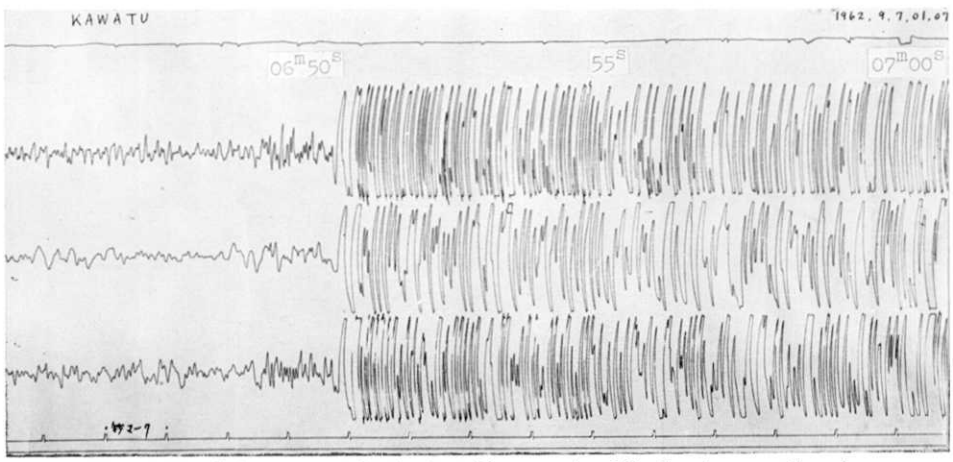

Fig. 5-40. Seismogram obtained at Kawazu for Miyake-zima earthquake.

Fig. 5-41. Seismogram obtained at shot point for Kawazu explosion.

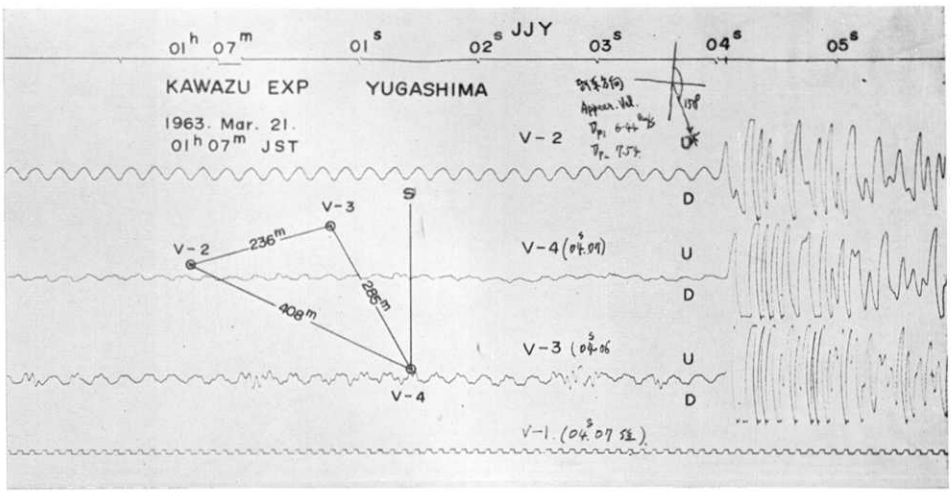

Fig. 5-42. Seismogram obtained at Yugasima for Kawazu explosion.

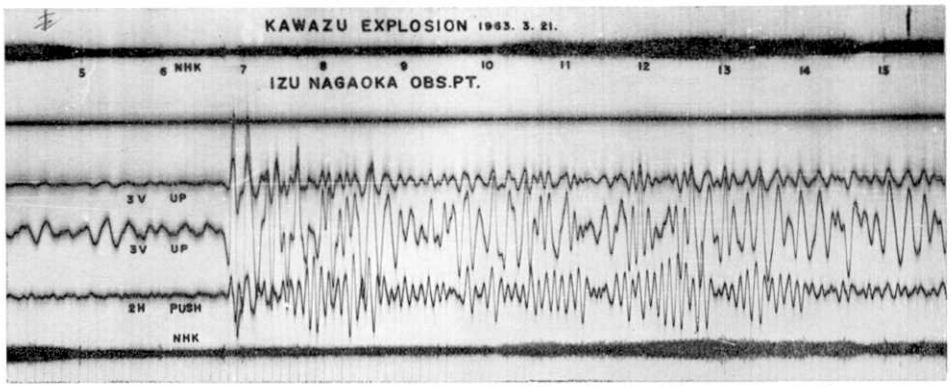

Fig. 5-43. Seismogram obtained at Izu-Nagaoka for Kawazu explosion.

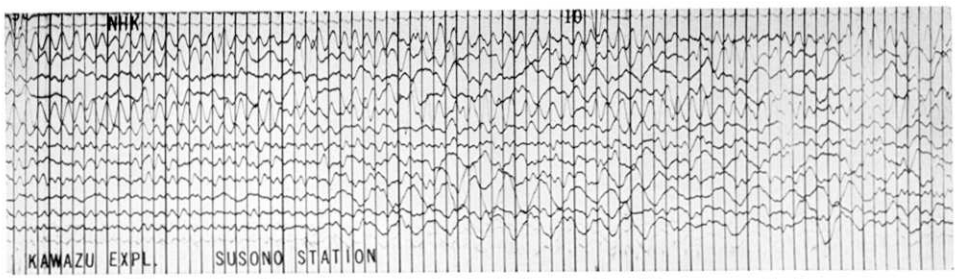

Fig. 5-44. Seismogram obtained at Susono for Kawazu explosion.

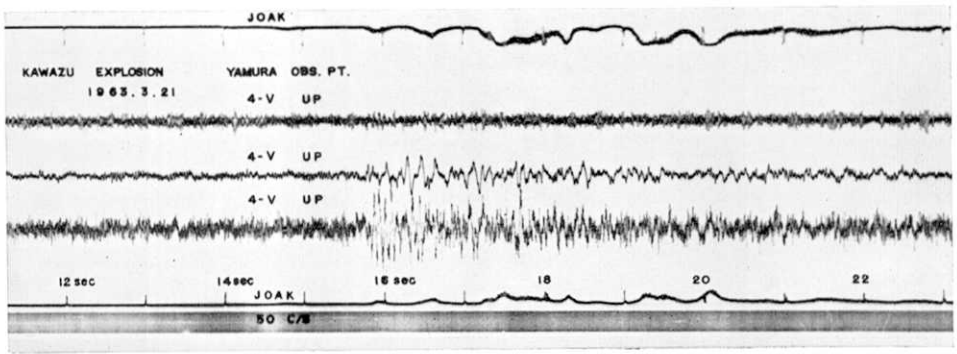

Fig. 5-45. Seismogram obtained at Yamura for Kawazu explosion.

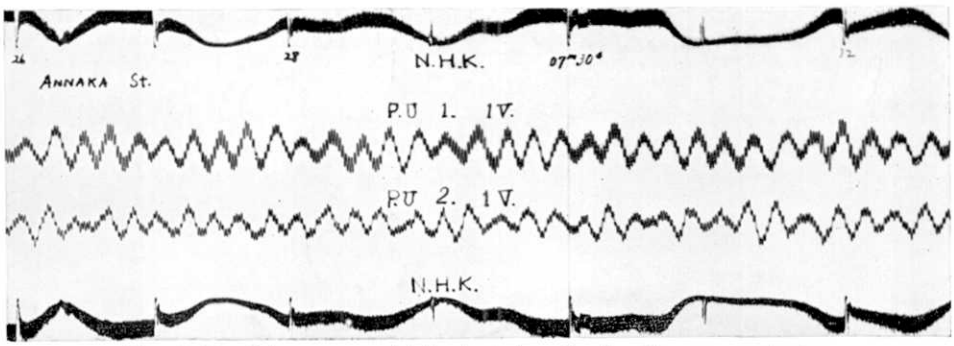

Fig. 5-46. Seismogram obtained at Annaka for Kawazu explosion.

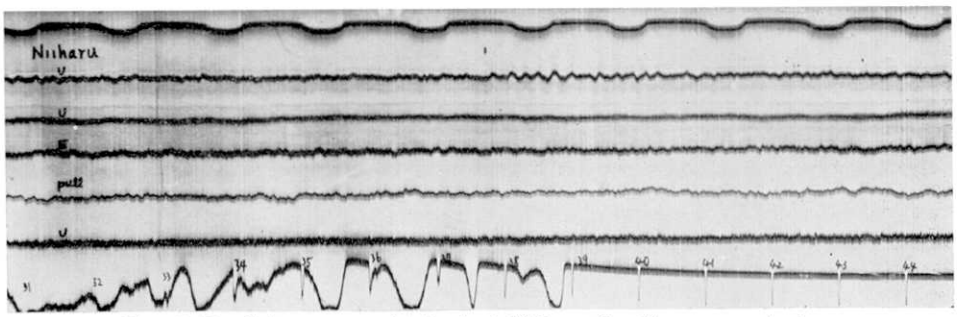

Fig. 5-47. Seismogram obtained at Niiharu for Kawazu explosion.

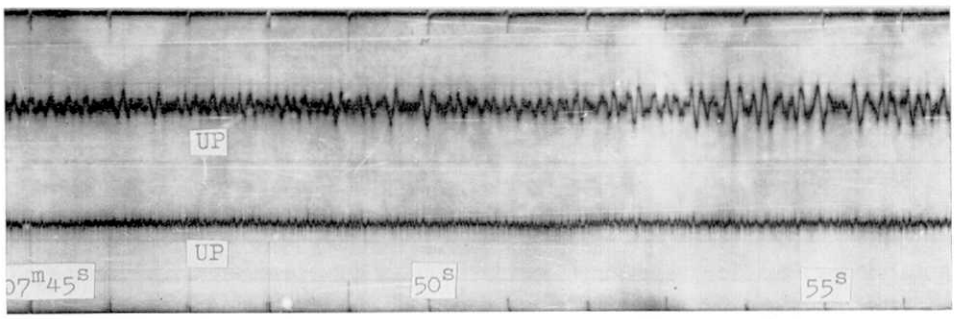

Fig. 5-48. Seismogram obtained at Yuzawa for Kawazu explosion.

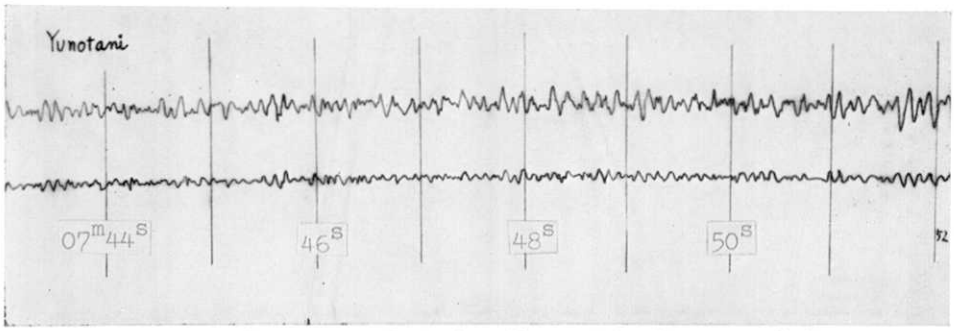

Fig. 5-49. Seismogram obtained at Yunotani for Kawazu explosion.

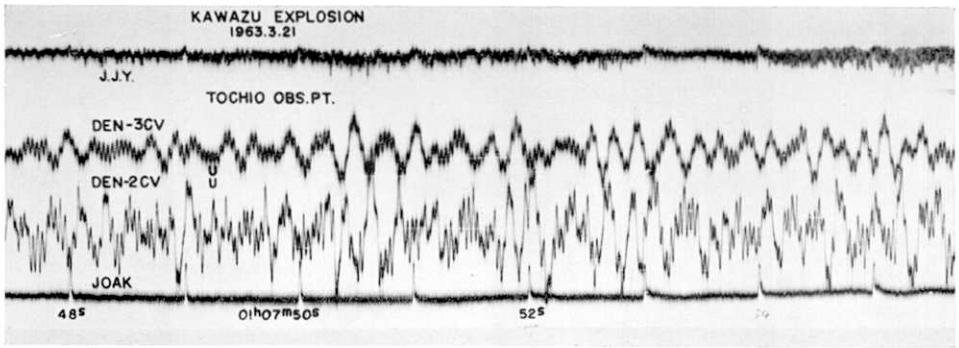

Fig. 5-50. Seismogram obtained at Totio for Kawazu explosion.

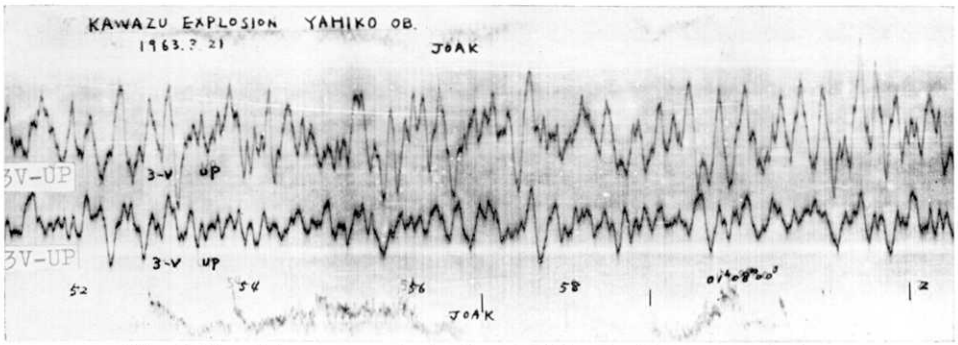

Fig. 5-51. Seismogram obtained at Yahiko for Kawazu explosion.

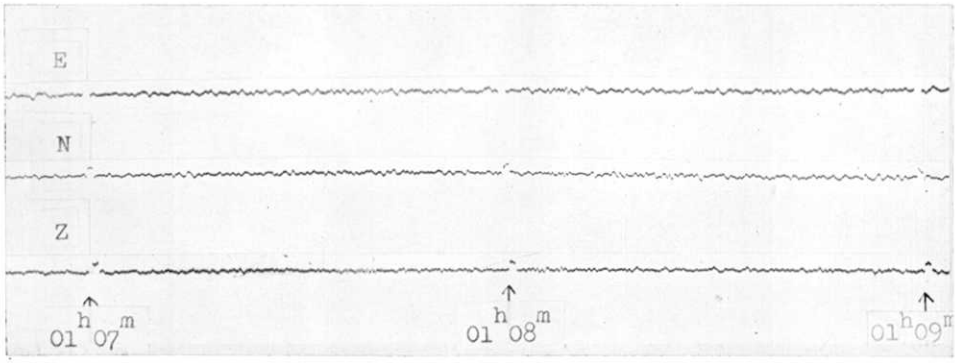

Fig. 5-52. Seismogram obtained at Matsushiro for Kawazu explosion.

In conclusion, sincere thanks are extended to members of the Research Group for Explosion Seismology for their helpful discussions and to Miss M. Gotô and Mrs. T. Huzita for their help in preparing the manuscript and diagrams.

---

27. 爆破地震動観測による本州中央部を南北に横断する測線上の地殻構造

第2部　地殻構造

北海道大学理学部地球物理学教室　堀田　宏
国立科学博物館　村内必典
東京大学地震研究所　宇佐美龍夫
東京大学地震研究所　嶋悦三
北海道大学理学部地球物理学教室　本谷義信
国立科学博物館　浅沼俊夫

第1部にのべた紫雲寺，安中，河津爆破および三宅島地震の地震動の観測結果を解析し，次のような東経 139°E に沿つた断面上における地殻構造を得た．各観測点での P 波初動から求められた走時曲線は，次のようなみかけの速度 (km/sec) と原点走時 (括弧の中，sec) を示す．

紫雲寺爆破：　1.64 (0.024)；5.83 (2.14)；6.73 (3.65)
安中爆破：　2.31 (0.020)；6.42 (1.67)；5.51 (0.48)
河津爆破：　2.83 (0.012)；6.00 (0.83)
三宅島地震：　6.13 ($6^m37^s.26$)；6.92 ($6^m39^s.38$)；7.69 ($6^m41^s.97$)

地殻は表層，第1層，第2層，マントルから成る．表層は各爆破点近くで上記の値をもち，深さは1～2km である．第1層の速度は，6.00 km/sec で湯の谷，五十沢附近で地表に出ている．また，その下面は，1°29′ の角度で南下りに傾き，紫雲寺での厚さは 11.8 km である．第2層は速度 6.82 km/sec である．この程度の速度をもつ層が観測され，その形状が求められたのはわが国で最初のことである．この層の下面，つまり，モホ不連続面の形状は一義的には求まらない．そこでマントル上部の P 波速度を 7.7～8.2 km の範囲で変化させた時のこの不連続面の様子をしらべた．この面は，紫雲寺附近で約 40 km の深さにあり，南下りで (勾配約 1～2°)，安中附近でもっとも深く，50～60 km くらいとなる．ここから先は南上りとなり，三宅島附近で深さ約 25～30 km となる．したがつて，第2層は南に行くにつれてうすくなり，三宅島附近では，ほとんどなくなる．この辺の事情を調べることは，将来に残された興味ある問題である．